Separation and Purification Technology 254 (2021) 117610

Contents lists available at ScienceDirect

Separation and Purification Technology

journal homepage: www.elsevier.com/locate/seppur

A two-step microengineered system for high-density cell retention from bioreactors

Maira Shakeel Syed[a], Christopher Marquis[b], Robert Taylor[a,c], Majid Ebrahimi Warkiani[d,e,*]

[a] School of Mechanical and Manufacturing Engineering, University of New South Wales, Sydney, NSW 2052, Australia
[b] School of Biotechnology and Biomolecular Science, University of New South Wales, Sydney, NSW 2052, Australia
[c] School of Photovoltaic and Renewable Energy Engineering, University of New South Wales, NSW 2052, Australia
[d] School of Biomedical Engineering, University of Technology Sydney, Sydney, NSW 2007, Australia
[e] Institute of Molecular Medicine, Sechenov First Moscow State University, Moscow 119991, Russia

ARTICLE INFO

Keywords:
Cell separation
Mini-hydrocyclone
Spiral microchannel
Mammalian cells
Microfiltration
Inertial microfluidics

ABSTRACT

Large-scale cell culture processes are required to produce biopharmaceuticals, cells for tissue engineering, and vaccine production while being effective in toxicity testing, gene therapy vector production for cancer research, and drug development. A growing trend in these industries, particularly for suspension cells, involves implementation of continuous cell perfusion processes, which require an aseptic, efficient, cost-effective, and reliable cell separation and retention scheme. Many cell separation techniques (membrane-based systems, lateral displacement devices, and acoustophoresis) have proven to be highly efficient, but suffer from issue of clogging and high cost, limiting their reliability, and thus, their overall feasibility. Some cell retention devices—those based on inertial microfluidics—offer high reliability (i.e., clog-free), but their efficiency reduces at higher cell concentrations. To overcome this apparent trade-off, we report the development of an integrated system consisting of two different membrane-less microfiltration techniques for cell separation from spent cell media. Although it could be adapted to numerous cell culture applications, this system was optimized and tested for suspension-adapted Chinese Hamster Ovary (CHO) cells. As the first step of the cell retention system, a miniaturised hydrocyclone was developed that could separate the cells with macroscopic volume processing rates (~200 mL/min). At this stage, up to 75% of the cells were isolated with minimal (< 5%) change in the viability. The remaining cells passed through the overflow of the device and entered to a multiplexed spiral microchannel system, where more than 90% of the remaining cells were recovered, yielding an overall efficiency of up to 95%. The proposed integrated system is thus ideal for continuous and high throughput cell retention even at high cell concentrations (~80 million cells/mL), which is in range of current need in the bioprocessing industry.

1. Introduction

Scale-up has always been a prominent issue of biopharmaceutical production. The rising demand to produce antibiotics, vaccines, therapeutics, and various testing and disease treatment applications around the world provides an impetus for developing new technologies to improve cell culture and retention processes. The commercial value of these biologics exceeds US$100 billion/year worldwide [1], with mammalian cell expression systems constituting the dominant production cell line of the biopharmaceutical industry. This is largely due to the growing trend of using monoclonal antibodies as therapeutic candidates [2]. For high-density cultivation of the suspended mammalian cells producing these antibodies, periodic/continuous replacement of growth media is required [3]. The development of fully continuous processing of mammalian cells has the potential to significantly reduce bio-manufacturing costs and improve product quality [4,5]. These systems would enable continual feeding of nutrients and continuous removal of waste, both of which can contribute to higher volumetric production and product concentration [4,6–8]. Several continuous systems have been proposed and tested in the past, including cell separation based on membrane filtration, gravitational settling, centrifugation, and acoustic wave separation, all which have some drawbacks [9,10]. Among these, the most successful approach seems to be using a hollow-fibre membrane either in Tangential Flow Filtration (TTF) [11] or Alternating Tangential-flow Filtration (ATF) configurations [10,12]. However, due to the deposition of cells and molecules, which leads to pore blockage, these membranes have a high risk of clogging and fouling [13]. In some ATF systems, the membranes

* Corresponding author.
E-mail addresses: maira.syed@unsw.edu.au (M.S. Syed), majid.warkiani@uts.edu.au (M.E. Warkiani).

https://doi.org/10.1016/j.seppur.2020.117610
Received 14 March 2020; Received in revised form 12 August 2020; Accepted 14 August 2020
Available online 25 August 2020
1383-5866/

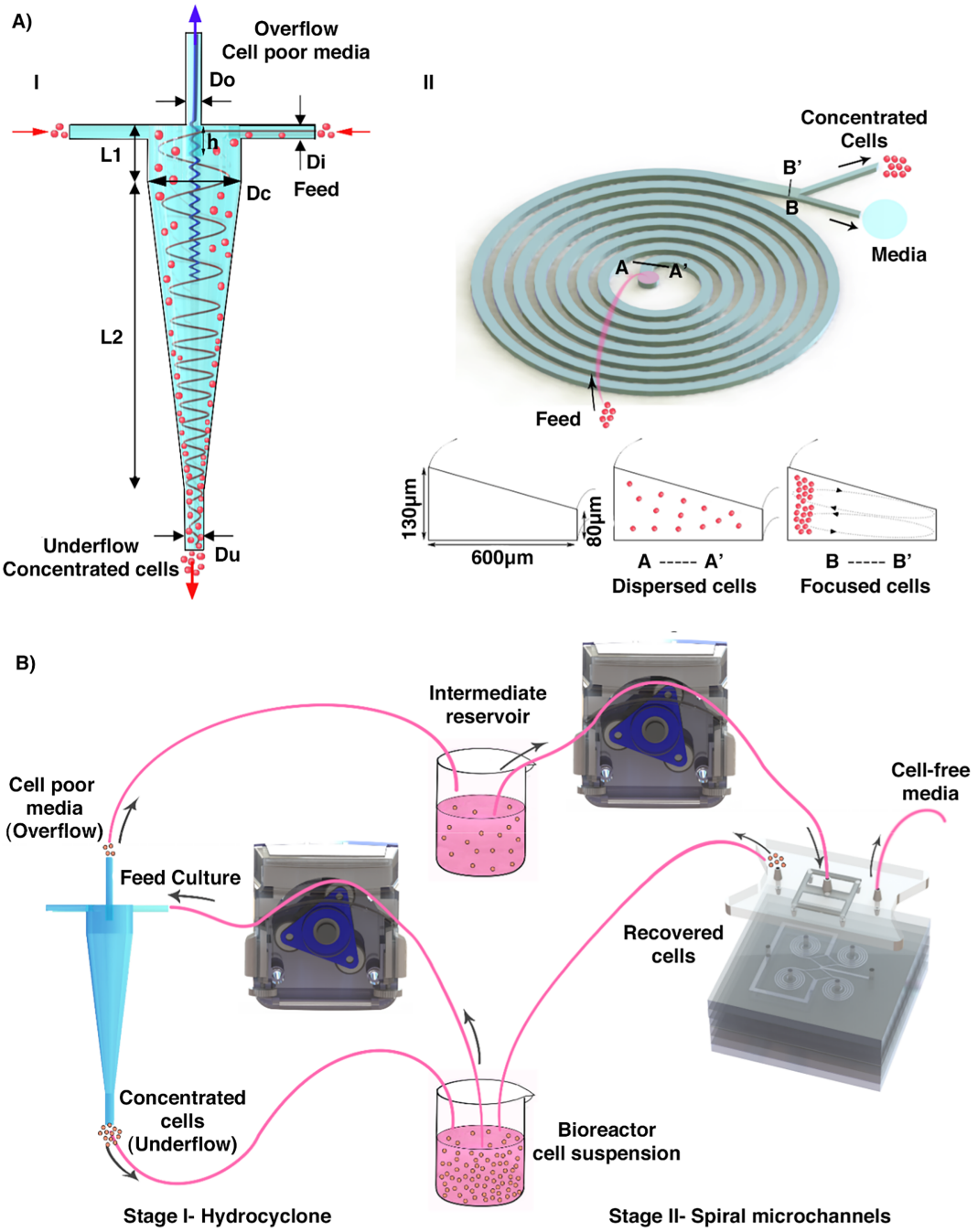

Fig. 1. (A) I. Schematic illustration of a micro-hydrocyclone showing the flow of particles inside the device. Gray curved line indicates the path followed by the particles, while the blue vortex shows the flow of fluid and finer particles. II. Working principle and schematic illustration of spiral microchannel. The inertial forces focus particles/cells close to the channel wall; (B) Schematic diagram of the integrated miniaturized hydrocyclone/spiral microchannel system. Cell culture is pumped into the hydrocyclone first for pre-sorting, and then the cell poor stream is pumped into the multiplexed spiral microchannel device for concentration.

are replaced by diaphragms [9,14], but the chances of fouling are still prevalent [9,15], thus reducing cell concentration and viability, permeate flow, as well as the protein recovery and productivity [16,17]. Therefore, there is still a requirement for an improved cell retention system that could separate the cells efficiently (> 90%), with high flowrates (> 100 mL/min) and at high concentration (> 10^7 cells/mL), to meet the demands of the biopharmaceutical industry [7,18].

Recently, microfluidic-based devices have gained prominence for their ability to control and focus particles and cells based on their size and morphology [19,20]. From the two major classes of microfluidic separation (e.g. active and passive), passive-separation devices are often favoured since they offer a low-cost and, perhaps, a more reliable solution as no external forces (aside from a fluid pump) are required [7]. Some of these techniques, such as microfiltration and centrifugation, are frequently utilized, but they are often slow and hard to scale-up [21]. One of the most successful passive methods for high-throughput cell sorting is inertial microfluidics [22]—a technique that focuses particles/cells laterally in a microchannel by utilizing a combination of hydrodynamic forces [23,24]. Inertial microfluidics based devices have previously been employed for circulating tumour cells (CTCs) isolation [25,26], malaria detection [27], mammalian cell separation [7], cell cycle synchronization [18], detection of bacterial spoilage from beer [28], and for culturing/sorting microalgae cells

[29]. Although a single microchannel cannot have commercially relevant flow rates, Warkiani et al. [18] showed that through device parallelization (an array of microchannels), it is possible to increase the overall flow throughput, up to 500 mL/min. However, the efficiency of the system dropped drastically at higher cell concentrations ($> 10^7$ cells/mL) and higher concentrations could even result in clogging due to channel blockage in such small hydraulic diameter channels.

To overcome these limitations, this study demonstrates an integrated system of two distinct separation techniques (placed in series) that—as a whole—could offer high-throughput processing of high cell density suspension cultures. As the first part of the system, we propose the application of a micro-hydrocyclone due to its high-throughput, low cost, and low maintenance requirements [30]. This part of the system takes advantage of the versatile and robust nature of the traditional macro-scale hydrocyclone separation device—a device with no moving parts. Hydroyclones have a long history of success in the chemical and mineral industries [31,32], the oil industry [33,34], food processing [35], irrigation [36], waste management [37,38], and biotechnology [39,40]. The use of hydrocyclones for mammalian cell separation has previously been shown as well [41–44]. However, those studies were limited to low cell densities (< 10 million cells/mL) [9,45]. Few propose that further development of these hydrocyclones, particularly if optimized to specifically suit mammalian cells, could make them competitive with conventional cell retention techniques [9]. Although there are several advantages to micro-hydrocyclones [46,47], accurately manufacturing them has been difficult. In our previous study, we demonstrated a 3D printed mini-hydrocyclone for harvesting microalgae cells [30]. Building upon this, the present study will further scale down the design to fabricate an optically transparent micro-hydrocyclone using 3D printing and softlithography. Since the efficiency of micro-hydrocyclones is relatively low, we hypothesize that if coupled with a multiplexed inertial microfluidics system of spiral microchannels, it may be possible to obtain the best features of both unit operations (high efficiency and high throughput). Thus, in this study we propose an integrated system which, for the first time, combines microfluidic-hydrocyclones and multiplexed microchannels, and demonstrates the performance of this system for the separation and retention of mammalian cells. Suspension-adapted Chinese Hamster Ovary (CHO-S) cells are used in this work as a model cell line, since they are commonly used in the industry for bulk production of monoclonal antibodies and other protein therapeutics. CHO cells are generally spherical in shape having an average size of 12 μm and thus the system proposed in this system can also be applied to other cell lines having similar properties. The size distribution and shape of the CHO cells are described in ESI (supplementary Section B).

2. Theoretical analysis and design

2.1. The hydrocyclone

The hydrocyclone utilizes a tangential injection of fluid pressure to create a rotational/swirl fluid motion inside its cylindrical-conical structure (Fig. 1A). The swirl creates a double vortex flow inside the hydrocyclone, with a low-pressure zone along the vertical axis. The outer, downward vortex is called the primary vortex (gray), and the inner, upward vortex is called the secondary vortex (blue). As particles pass through the hydrocyclone, they experience three forces: 1) The centrifugal force (F_C) in an outward radial direction due to the tangential velocity (pushing the particles to the wall as a function of their size, shape, and density). 2) The buoyant force (F_b) in an inward radial direction that is due to the density difference of the fluid and the particle. 3) The drag force (F_d) having the direction inward or outward, depending on the direction of the particle's radial velocity, opposing any particle velocity components that are not aligned with the flow velocity due to the fluid viscosity. The relative magnitude of these forces a particle experiences depends on the particle size and shape as well as the cyclone geometry and flow rate (i.e., turbulent flow intensity) [48]. The particles for which F_C is dominant, follow the main flow in the primary vortex out of the underflow (bottom of the device). Whereas very fine and neutrally buoyant particles remain dispersed and entrained by the fluid due to the minuscule magnitude of these forces and thus exiting through both outlets (overflow and underflow).

The diameter of the cylindrical part, D_c, represents the key parameter on which other dimensions are based (Fig. 1AI) [49,50]. Two of the most commonly used design ratios for hydrocyclones are Bradley and Reitema's ratios, with Bradley's ratio being more suitable for lower particle cut-size (d_{50}) [51]. Therefore, in this study, the hydrocyclone design was based on Bradley's geometrical ratios with a few variations in the outlet dimensions and overall length of the device to modify the design for better separation. For more details on the specific design used in this study, please see the geometrical dimensions shown in supplementary Table S1.

2.2. The spiral microchannel

Microparticles or cells suspended in a fluid flowing in a straight microchannel tend to focus at certain lateral positions inside the channel. This focusing, known as inertial focusing, occurs due to the net lift force (F_L), which is a balance between shear gradient-induced and wall-induced lift forces [22,52]. Curved channels, such as spiral microchannels, introduce a secondary flow of two counter-rotating flows called Dean vortices. These vortices are perpendicular to the direction of the main flow and induce an additional drag force (F_D) on particles. Both of these forces are dependent on particle size and Reynolds number (Re), and the particle equilibrium position along the channel is determined by the net balance of these forces [22].

For this study, a trapezoidal cross-section channel was designed with 8 loops, as is shown in Fig. 1AII. This microchannel has a single inlet and two outlets. The channel is 600 μm wide throughout, and it has an inner height of 80 μm and an outer height of 130 μm. A multiplexed system containing 40 such channels bonded in different layers was tested as well. This design of spiral microchannel was chosen due to its capability to efficiently separate the mammalian cells, albeit with limited cell density (up to 30×10^6 cells/mL) and throughput (~50 mL/min) [18].

3. Materials and methods

3.1. Hydrocyclone fabrication

The mini-hydrocyclone was fabricated using our previously developed approach (based on additive manufacturing, which shows a great promise in fabrication of microfluidic devices [53–56], but this time in a Polydimethylsiloxane (PDMS) block. In short, the CAD model of the mini-hydrocyclone was developed using SolidWorks 2017 and was 3D printed with SolidscapeVR MAX2 printer (Solidscape, Inc., Merrimack, NH, USA) in wax mixtures. Due to long, thin overhanging structures, some additional supports were added to the exterior of the design to strengthen these without affecting the hydrocyclone's main features. This type of printer uses a combination of additive and subtractive manufacturing to make an object by developing successive 2D layers. Each layer was created using a direct writing technique depositing molten wax droplets which solidify by cooling on impact. The device was printed at 25 μm resolution in ~7 h; however, finer settings (up to 6 μm) could also be used (if desired), but at the expense printing time (e.g., it would take 5 times longer). The final model was printed with a 3Z Model material (a propriety wax mixture from Solidscape, Inc.) for the main structure and with a 3Z Support material (Solidscape, Inc.) for voids and gaps. The support material was melted in a solvent at 60 °C and the final product was placed on a petri dish for molding. PDMS (Sylgard 184 Silicone Elastomer Kit, Dow Corning) mixed in a ratio 7:1 of base: curing agent was pre-degassed in a vacuum chamber for

molding around the product. Note that a higher mixing ratio was used (than the usual 10:1 ratio) to make the PDMS harder and less deformable to the relatively high pressure/flow rates inside the hydrocyclone. The PDMS was then poured over the wax structure in the petri dish and subsequently degassed once more and cured at 65-75 °C for a couple of hours. The cured PDMS containing the wax model was then cut tangential to the inlets and outlets of the structure. Finally, the 3D printed wax model was melted in an oven (at melting temperature 95–120 °C) and the device was flushed with acetone to remove residual wax. The final form of the molded hydrocyclone is shown in supplementary Fig S3(B).

3.2. Spiral microchannel fabrication

The spiral microchannels' mold was milled from an aluminum block using a micro-milling technique. Channels were also fabricated with PDMS using softlithography. Degassed PDMS, mixed in a 10:1 ratio of the base and curing agent, was poured onto the aluminum mold. After 2 h of baking inside an oven at 65 °C, the PDMS was peeled off, and fluidic access holes were punched using a Uni-Core™ puncher (Sigma-Aldrich Co. LLC. SG). Finally, the PDMS was irreversibly bonded to a thick PDMS slab using an oxygen plasma cleaner (PDC-002, Harrick Plasma, Ossining, NY).

For fabrication of the multiplexed system, the aluminum mold contained positive pattern of 4 spiral channels connected systematically, as described by our group previously [18]. Ten layers of these channels were then bonded together with an oxygen plasma cleaner, such that the inlet and outlets of all the layers were aligned. The final multiplexed system contains 40 spiral microchannels and a total of 4 inlets and 2 outlets (shown in supplementary Fig S3(C)). A 3D printed flow splitter (printed with Projet 3500 HD Max, 3D System) was also designed for equal distribution of flow to every spiral in each layer. For the outlets, tubing was directly inserted into the punched holes, to form liquid-tight seals.

3.3. Cell culture

The CHO.K1 cells suspension cells (CHO-S) were cultured in 250 mL disposable shake flasks (Polycarbonate Erlenmeyer Flask, Corning, USA) on a shaker at 250 rpm. The cells were cultured in commercial culture media (CD CHO, Thermo Fisher Scientific, USA), supplemented with 1% Glutamax (GlutaMAX™, Thermo Fisher Scientific, USA), antibiotics, and Gibco anti-clumping agent. The culture was maintained at 37 °C in a humidified atmosphere containing 5% (v/v) CO_2. The cells were analyzed (cell count and viability) daily using a benchtop cytometer (TALI, Thermo, USA) and passaged every third day. The cells were seeded at the initial concentration of 0.5×10^6 cells/mL and upon the onset of the stationary growth phase (2–3 days), as determined by cell counting and viability analysis, the cells were fed to the microchannel for separation tests.

3.4. Experimental setup and procedure

Before testing with the CHO cells, both devices were characterized independently by experiments with surrogate polystyrene (PS) microbeads at different flow rates. For the hydrocyclone experiments, PS particles in dry powder form (Cospheric, USA) were used for preparing high particle concentrations by mixing the 12 μm particles in AutoMACS buffer (MiltenyiBiotec, Germany) consisting of 1 × phosphate buffered saline (PBS), 2 mM EDTA supplemented with 0.5% bovine serum albumin (BSA). The 12 μm particle size was chosen to mimic the average CHO cell size. To homogenize the particles, the suspension was sonicated for two hours in a cold-water bath.

The suspension was mixed on a magnetic stirrer and was pumped into the mini-hydrocyclone using a peristaltic pump (Masterflex Easy-Load® II, Cole Palmer, USA). The discharge from both outlets (underflow and overflow) was collected in different centrifuge tubes, and particle concentration before and after separation was determined with a hemocytometer. Based on these particle counts, the efficiency of hydrocyclone can determined by Eq. (1).

$$\textit{Separation Efficiency } (E) = 1 - \frac{X_o}{X} \tag{1}$$

where X_o and X are the concentrations of overflow stream and the feed, respectively. The hydrocyclone was characterized at different flow rates and concentrations. For each experiment, three replicates were obtained with five PDMS hydrocyclones of same design to ensure repeatability of the results.

Similarly, the spiral microchannel device was also tested with fluorescent PS microbeads (Fluoresbrite® Microspheres, Polysciences Inc, Singapore). For the aim of characterization, a single spiral microchip was placed on an inverted epifluorescence microscope with a CCD camera (Olympus IX73 microscope and Olympus DP80 camera, Olympus Inc., USA). The particle suspensions were injected into the channel using a syringe pump (Cole Palmer, USA). Then, the fluorescent particle traces were observed at the point of bifurcation of the channel at various steady flow rates ranging from 0.5 to 2 mL/min. Finally, the multiplexed system of spiral microchannels was tested with the microbeads at flow rates of 20 to 100 mL/min using a peristaltic pump. Samples were collected from the system outlets, and particle counts were obtained with a hemocytometer.

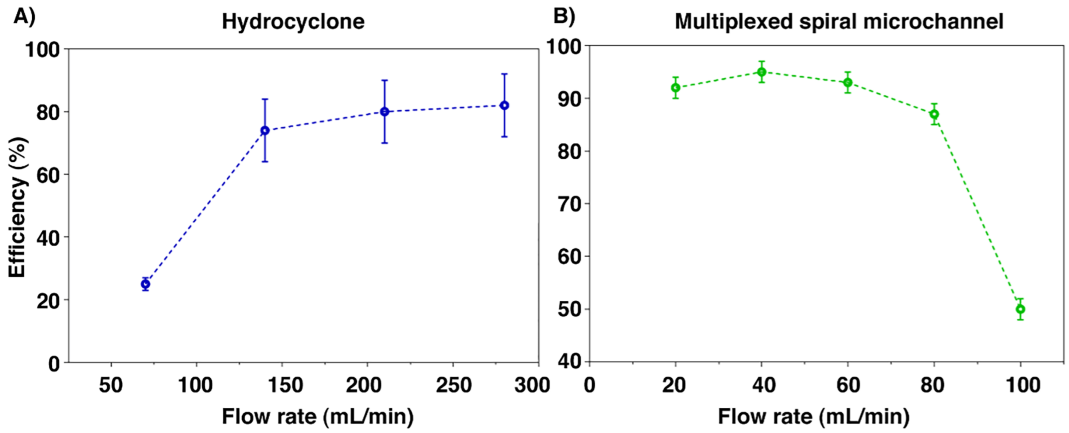

Fig. 2. (A) The results of separation of 12 μm PS microbeads for the individual characterization of mini-hydrocyclone at different flow rates. (B) Individual characterization of the multiplexed system of spiral microchannels at varying flow rates.

3.5. Tests with CHO cells

After the characterization of both devices with the microbeads, the devices were first tested individually with the CHO cells, and then the scheme for an integrated system was developed (Fig. 2). As compared to microbeads, using real cells necessitates a few more constraints on the testing. Contamination can be a major concern, so the tests were performed in a biosafety cabinet, and the devices and tubing were autoclaved and flushed (with 70% ethanol for 1 h and then sterile distilled water) before each test to ensure sterility of the system.

3.5.1. Hydrocyclone experiments

In order to check the effectiveness of hydrocyclone for separation of cells, the designed hydrocyclone was retested for CHO cells. Similar to particle testing, the cell culture was fed into the hydrocyclone via a peristaltic pump at different feed flow rates, and samples were collected for counting and cell viability analysis. In addition to flow rate characterization, the hydrocyclone was also tested at varying cell densities. As the maximum cell density achievable using the CD CHO media is restricted to $\sim 3 \times 10^6$ cells/mL [57,58], thus, several flasks of the cells were combined after centrifugation to obtain high cell concentrations of $\sim 40 \times 10^6$ cells/mL.

3.5.2. Multiplexed spiral microchannel experiments

After testing the hydrocyclone, the parallelized system of 40 spiral microchannels was tested with the cells, in a similar way as described in Section 3.4 for the microbeads. The samples were obtained for the feed culture, and the outlets were analyzed for cell counts and cell viability.

3.5.3. Cell viability analysis

Cell sizes, concentrations, and viabilities were measured by an automated image-based cytometer and analyzer (TALI™, Thermo, USA). For cell viability analysis, a 100 μL sample was stained with 1 μL of Propidium Iodide dye and incubated for 2–5 min in the dark. Next, 25 μL of the stained sample was placed on the TALI analysis slides and loaded into the analyzer. For each measurement, 13 images were obtained from different fields of view, based on which the cell size, viability, and concentration were determined. For verification, the traditional Trypan blue exclusion test was also performed using a hemocytometer and results were found to be in agreement with results obtained using the TALI.

3.6. Development of two-step integrated system

Finally, the two-step scheme for the separation of CHO cells (at high cell densities) was developed consisting of the micro-hydrocyclone and the multiplexed spiral microchannel system (Fig. 1B). The cell-rich stream from the underflow was recirculated back to the feed flask, whereas the overflow was collected in a middle reservoir flask. From this reservoir flask, the cell-poor media from the hydrocyclone overflow was pumped into the multiplexed spiral channel device. The inner outlet stream from spiral channels (which is rich in cells) was directed back into feed flask, while the cell-free stream from the outer outlet is collected separately. Samples were taken from initial culture flask, hydrocyclone outlets, spiral microchannel outlets, and the final culture flask for cell counts and viability analysis.

4. Results and discussion

The results obtained for the individual performance of the devices for microbeads as well as the CHO cells are provided in the sections below. Furthermore, it is also demonstrated how the overall performance is affected by combining the micro-hydrocyclone and spiral microchannel in series to form an integrated system for cell separation.

4.1. Tests with surrogate microbeads

As stated above, the first performance test for the hydrocyclone was carried out using 12 μm microbeads to mimic CHO cells. A remarkable increase in separation efficiency was observed as the feed flow rate increased from 60 mL/min to 150 mL/min (Fig. 2A). This was due to the exponential increase in the magnitude of centrifugal forces acting on the particles as the feed tangential velocity increases [30]. However, it is also worth noting that the curve flattened beyond a flow rate of 150 mL/min, which is because of the short-circuiting of flow to the overflow without flowing into the hydrocyclone body. Another reason is the higher degree of turbulence inside the hydrocyclone that disturbs the fluid motion, therefore, flowrates higher than 300 mL/min would result in decrease of efficiency rather than improving it. Hence, between the flow rates of 150 and 300 mL/min, the separation efficiency of the hydrocyclone remained between 75 and 80%. This suggests an optimum flowrate range for separation of the 12 μm microbeads or CHO cells, however, loss of 20–25% of microbeads/cells in the overflow is indicated. Therefore, use of a secondary device is reuired to supplement this loss. The particle count micrographs for underflow and overflow samples obtained from the hemocytometer are shown in Fig. S4A.

Similarly, for the characterization of the spiral microchannel, the trajectories of fluorescent PS microbeads were visualized under the microscope (Supplementary Fig. S2 A) for a single spiral channel before doing multiplexing. At low flow rates (i.e., $Q \leq 0.5$ mL/min), microbeads remained dispersed in the channel. By increasing the flow rate, the focusing band becomes sharper at $Q = 1$ mL/min, such that almost all of the particles were directed to the inner outlet. Upon further increasing the flow rates, however, due to the influence of F_D, the focusing band shifted gradually towards the outer half of the channel, until at $Q = 3$ mL/min, particles exited partly through both outlets. Thus, based on these evaluations, flow rates between 1 and 2 mL/min were deemed to be the most suitable for the efficient separation of cells.

Next, the multiplexed spiral microchannel system was also tested with the same microbeads. The particle count from the inlet and outlets showed a similar trend of separation as for the single spiral microchip. The separation efficiency for the total feed flow rate between 30 and 60 mL/min, remained higher than 90%, reaching upto 98% at 40 mL/min (Fig. 2B). Above 60 mL/min there was a marked drop in the separation efficiency of the device until it dropped to 50% at 100 mL/min. Further increase in the flow rate would allow focusing of microbeads towards the outer wall. However, as more than 60% of the fluid flows through the outer outlet, focusing the particles near inner wall should be better for achieving higher cell concentration in the outlet.

4.2. Tests with CHO cells

Based on the optimum flow conditions determined through the surrogate microbead studies (Section 4.1), similar tests were repeated with the CHO cells (average cell size: 12 μm). As mentioned above, all the experiments were conducted on the 2nd day of cell culture during the cell's stationary growth phase. The tests were first performed with both devices separately, and then, the integrated system was investigated.

4.2.1. Hydrocyclone results

To determine the effect of high shear forces inside the hydrocyclone, the cells were pumped through over a range of flow rates. The device separation efficiency and viability of the cells for both outlets were analysed at each flow rate (Fig. 3A). The hydrocyclone efficiency curve for the CHO cells was found to be in close agreement with results obtained with the surrogate microbeads, up to the total feed flow rate of $Q \leq 200$ mL/min. For these flow rates, no signs of cell damage were observed. A maximum efficiency of up to 78% was found at 200 mL/

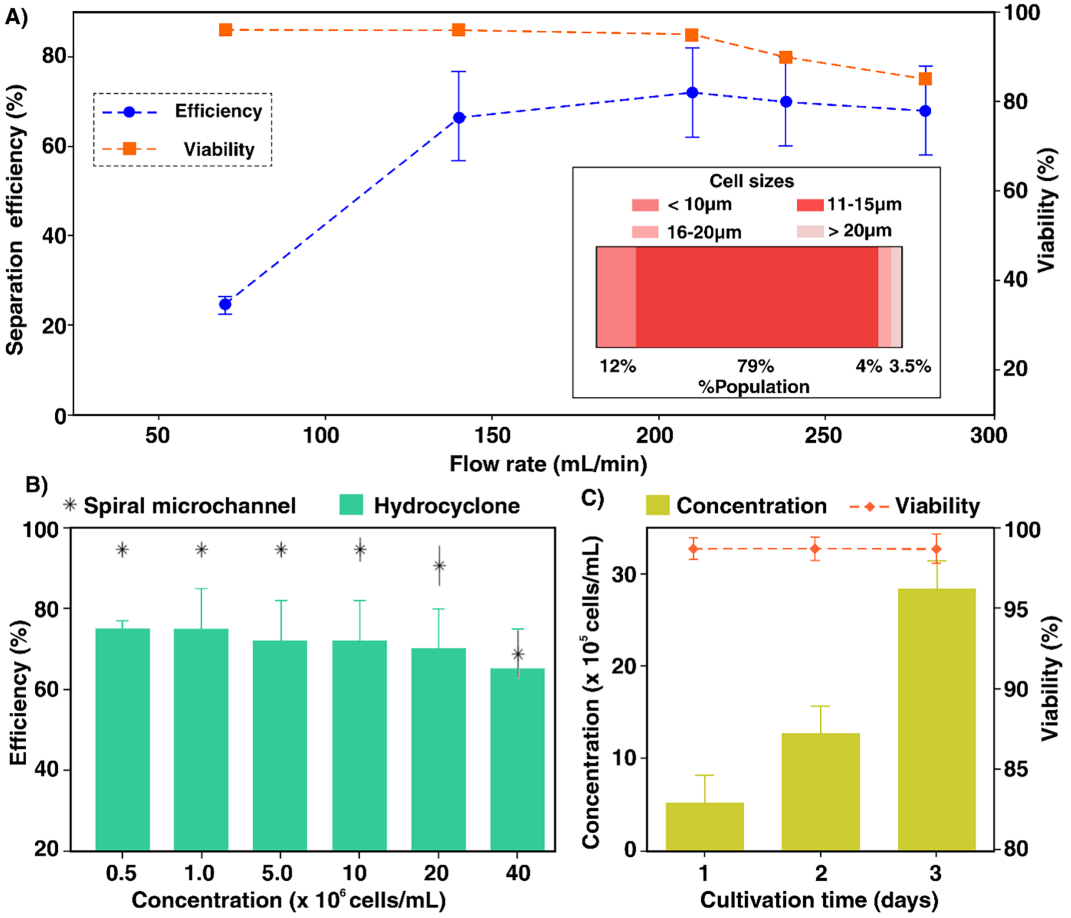

Fig. 3. Experimental results for the CHO cells: (A) Plot of separation efficiency and cell viability against various flow rates using only the hydrocyclone; (B) Efficiency plot for a range of cell concentrations between 0.5 million and 40 million cells/mL for both the hydrocyclone (bar chart) and the spiral microchannel (dot plot- data obtained from Kwon et al. [7]). The efficiency of both devices reduces at 40 million cells/mL; (C) Cell proliferation analysis after recirculation through the system. Cells doubled normally every 24, results indicate that cell viability was not compromised after passing them through the integrated system.

min. However, at higher flow rates, the cell viability dropped to ~85% at 280 mL/min, and the separation efficiency also decreased to 62%. The increasing shear forces at high flow rates, i.e., Q > 220 mL/min, did damage some of cells which was observed through their size shrinkage and shape deformation. Hence, as separation is dependent on cell size and shape, these damaged/lysed cells remained dispersed inside the hydrocyclone, and the efficiency decreased.

A flow rate of Q = 200 mL/min was found to be optimal, offering the highest efficiency as well as no drop in cell viability. For further confirmation of minimal cell damage through the hydrocyclone, samples from each outlet were collected and inoculated to check the cell proliferation capacity. The daily growth of the cells was monitored until they grew to their maximum concentration (Fig. 3C). The cells were seeded at 2.5 × 10^5 cells/mL on the day zero with 97% cell viability. The cells doubled every 24 h until the maximum recommended cell density (2.5–3 × 10^6 cells/mL for CD CHO media [57]) was reached on day 3 with same cell viability. As the cells grew normally after passing through the hydrocyclone at Q = 200 mL/min, all the further experiments would be performed at this flow rate.

Finally, to assess the performance of the hydrocyclone at higher cell densities, as required by the biomanufacturing industry, the device was tested at cell densities up to 40 × 10^6 cells/mL (Fig. 3B). For the concentrations up to 15 × 10^6 cells/mL, the separation efficiency of the hydrocyclone was found to be constant at ~78% at Q = 200 mL/min. However, there was a decline in efficiency of about 10–15% for a cell density of 40 × 10^6 cells/mL. Nevertheless, with the current results, we could successfully demonstrate that our designed hydrocyclone can be used efficiently with ultra-high throughputs as compared to other reported microfluidic cell retention techniques.

4.2.2. Multiplexed spiral microchannel results

Next, the tests with the CHO cells were repeated with the multiplexed spiral system. The separation efficiency trend matched well with the microbead results as well as with results reported by Warkiani et al. [18] and Kwon et al. [7] for the same device (Supplementary Fig. S2 B). The efficiency peaked at flow rate of 40 mL/min with upto 95–97% separation efficiency. Slight difference in sepation efficiency for the cells was observed, as compared to the microbeads, which is attributed to the variation in size in the cell population (supplementary Fig. S1). The influence of cell density on the separation of device (obtained from Kwon et al. [7]) has been compared with the hydrocyclone in Fig. 3B. The spiral microchannel system works efficiently for concentrations up to 20 × 10^6 cells/mL; however, for the concentrations higher than 26.5 × 10^6 cells/mL, the efficiency dropped below 83%. The drop in efficiency is due to the wider focusing bands that resulted in cell loss to the outer outlet of the device. Thus, for the processing of high cell concentrations, we coupled the system with micro-hydrocyclone, discussed in the section below.

4.3. Two step integrated system

In order to overcome and recapture the cells lost through the overflow of the hydrocyclone and through the outer outlet of the multiplexed spiral microchannel at high cell densities, the two devices

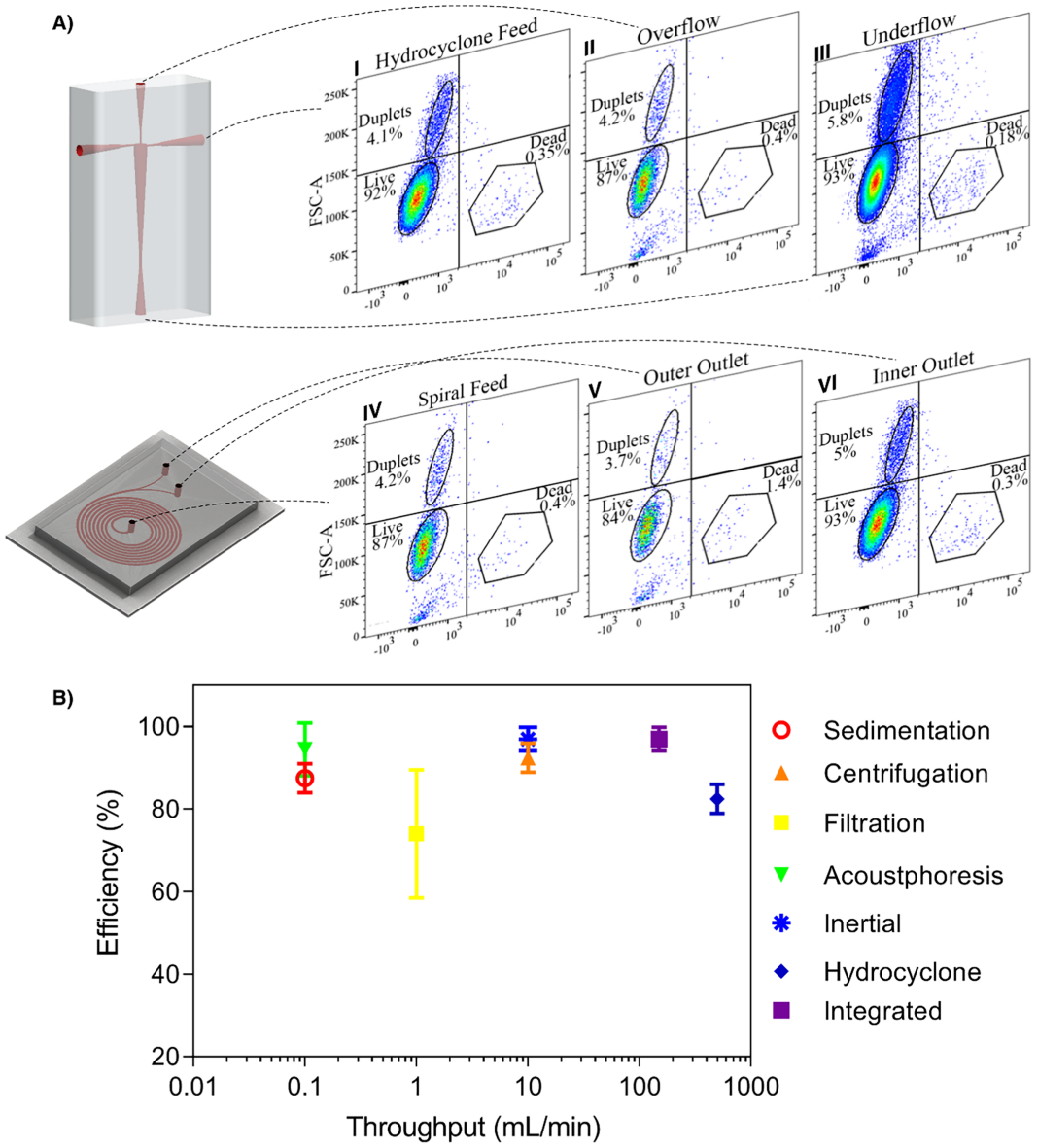

Fig. 4. (A) Flow cytometer plots showing cell densities and viability of the cells for different samples I. Hydrocyclone Feed, II. Overflow, III. Underflow, IV. Spiral Feed V. Outer outlet VI. Inner outlet, obtained from the timed flow cytometer run of 30 s; (B) Efficiency and throughput comparison of our integrated system with other techniques.

were integrated (Fig. S3 A). Both devices were run at the optimal flow rates obtained from the flow rate characterization in the previous sections (i.e., 200 mL/min for hydrocyclone and 40–60 mL/min for the spiral system). As the separation was done in two stages in series, both devices shared the load of each other and which led to better overall separation efficiency at higher concentrations (Fig. 4A). In this pilot-scale study, the proposed integrated system was tested up to the maximum concentration of 40 $\times$ 10^6 cells/mL; however, based on the current results, the cell concentration limit for the system can be estimated. The system can work with a composite efficiency of up to 90% until the cell concentration of the overflow reaches ~29 $\times$ 10^6 cells/mL. As shown earlier (Fig. 3B), beyond this concentration, the effciency of the spiral microchannels (stage II) decrease gradually. For the overflow concentration of ~29 $\times$ 10^6 cells/mL, considering atleast 65% efficiency of the hydrocyclone (stage I), initial concentration of up to 83 $\times$ 10^6 cells/mL can be calculated (using Eq. (1)). Hence, it can be concluded that the system has the potential for overall cell separation efficiency of 90% for cell densities up to 83 $\times$ 10^6 cells/mL, which is in the range of current need in the bioprocessing industry.

Thus, our proposed integrated system has the capability to be employed as an efficient and high throughput cell retention process suitable for high cell densities to meet industrial cell culture demands. However, there is room for future work on these types of integrated systems, namely: A) A larger scale study is needed to further stretch the upper limit of cell concentrations, ideally up to 100 million cells/mL; B) A fresh media supply to be added to the bioreactor vessel, to create a truly continuous perfusion process; and C) Longer term testing should be conducted with automated valving and pumping mechanisms to allow system configuration modification as required. D) Implementation of system for other cell lines for numerous applications such as microalgae dewatering, separation or sorting of blood cells and blood plasma separation.

5. Conclusions

In this study, a systematic investigation was conducted to develop an integrated microfluidic cell separation system which can achieve both high throughput and efficiency. The system was characterized

with PS microbeads and tested with CHO cells to showcase its potential for a wide range of cell separation applications. For the first stage of separation, a miniaturized hydrocyclone was developed using additive manufacturing and soft lithography. At the optimized flow rate of 200 mL/min, up to 80% of the cells were separated at this stage, with no drop in cell viability. The remaining cells were recaptured using the multiplexed system of spiral microchannels as the second stage of separation. Therefore, the overall efficiency of the system remains at more than 90% at the estimated cell density of ~80 million cells/mL. Overall, the findings from this study open up a new, low-cost, high throughput, and efficient method for cell separation that could be extended to various other biotechnological fields, such as plasma separation from blood, dialysis as well microalgae harvesting, and dewatering for biofuel production.

CRediT authorship contribution statement

Maira Shakeel Syed: Methodology, Software, Validation, Writing - original draft, Writing - review & editing. **Christopher Marquis:** Validation, Supervision, Writing - review & editing. **Robert Taylor:** Validation, Supervision, Funding acquisition, Writing - review & editing. **Majid Ebrahimi Warkiani:** Conceptualization, Methodology, Validation, Supervision, Funding acquisition, Writing - review & editing.

Declaration of Competing Interest

The authors declare that they have no known competing financial interests or personal relationships that could have appeared to influence the work reported in this paper.

Acknowledgments

M.S would like to acknowledge the support of Australian Government Research Training Program Scholarship for conducting this research at UNSW and also Biological Resources Imaging Laboratory (BRIL) for providing equipment for flow cytometery experiments. R.A.T. would like to acknowledge the support of the Australian Research Council (DE160100131). This research work was supported by the Australian Research Council through Discovery Project grants (DP170103704 and DP180103003). M.E.W. would like to acknowledge also the support of the National Health and Medical Research Council via the career development fellowship (APP1143377).

Appendix A. Supplementary material

Supplementary data to this article can be found online at https://doi.org/10.1016/j.seppur.2020.117610.

References

[1] G. Walsh, Nat. Biotechnol. 32 (2014) 992.
[2] M.-E. Lalonde, Y. Durocher, J. Biotechnol. 251 (2017) 128–140.
[3] L.R. Castilho, R.A. Medronho, in Tools and Applications of Biochemical Engineering Science, Springer Berlin Heidelberg, Berlin, Heidelberg, 2002, pp. 129-169, DOI: 10.1007/3-540-45736-4_7.
[4] A.L. Zydney, Curr. Opin. Chem. Eng. 10 (2015) 8–13.
[5] P. Moazzam, H. Tavassoli, A. Razmjou, M.E. Warkiani, M. Asadnia, Desalination 429 (2018) 111–118.
[6] J.N. Warnock, M. Al-Rubeai, Biotechnol. Appl. Biochem. 45 (2006) 1–12.
[7] T. Kwon, H. Prentice, J.D. Oliveira, N. Madziva, M.E. Warkiani, J.-F.-P. Hamel, J. Han, Sci. Rep. 7 (2017) 6703.
[8] W. Veena, G. Rahul, B. Kevin, J. Sujit, C. Daniel, S. Elizabeth, J. Timothy, W. Jason, Y. Marcella, W. Benjamin, M. Jean, K.K.P.H. Chris, Z. Weichang, R. Frank, K. Konstantin, Biotechnol. Bioeng. 109 (2012) 3018–3029.
[9] R. Patil, J. Walther, Springer Berlin Heidelberg, Berlin, Heidelberg, pp. 1-46, DOI: 10.1007/10_2016_58.
[10] V. Chotteau, in: Animal Cell Culture, ed. M. Al-Rubeai, Springer International Publishing, Cham, 2015, pp. 407-443, DOI: 10.1007/978-3-319-10320-4_13.
[11] F. Carstensen, A. Apel, M. Wessling, J. Membr. Sci. 394–395 (2012) 1–36.
[12] K. William, S. Jennifer, Z. Di, F. Gang, L. Mathew, C. Jason, K. John, B. Ravinder, Biotechnol. Prog. 30 (2014) 1291–1300.
[13] H. Fröhlich, L. Villian, D. Melzner, J. Strube, Chem. Ing. Technol. 84 (2012) 905–917.
[14] Z.A. L., Biotechnology and Bioengineering 113 (2016) 465–475.
[15] H.S. Ramesh, S.A. Kumar, M.V. Vilas, J. Chem. Technol. Biotechnol. 92 (2017) 732–740.
[16] D. Chee Furng Wong, K. Tin Kam Wong, L. Tang Goh, C. Kiat Heng, M. Gek Sim Yap, Biotechnol Bioeng 89 (2005) 164–177.
[17] C.D. Gregory, J.D. Pound, A. Devitt, M. Wilson-Jones, P. Ray, R.J. Murray, mAbs 1 (2009) 370–376.
[18] M.E. Warkiani, A.K. Tay, G. Guan, J. Han, Sci. Rep. 5 (2015) 11018.
[19] A. J. C. S. C. Hur, in: Micro- and Nanomanipulation Tools, DOI: doi:10.1002/9783527690237.ch1.
[20] S. Razavi Bazaz, A. Mashhadian, A. Ehsani, S.C. Saha, T. Krüger, M. Ebrahimi Warkiani, Lab Chip 20 (2020) 1023–1048.
[21] P. Sajeesh, A.K. Sen, Microfluid. Nanofluid. 17 (2014) 1–52.
[22] J. Zhang, S. Yan, D. Yuan, G. Alici, N.-T. Nguyen, M. Ebrahimi Warkiani, W. Li, Lab Chip 16 (2016) 10–34.
[23] M. Rafeie, J. Zhang, M. Asadnia, W. Li, M.E. Warkiani, Lab Chip 16 (2016) 2791–2802.
[24] D. Di Carlo, Lab Chip 9 (2009) 3038–3046.
[25] M.E. Warkiani, G. Guan, K.B. Luan, W.C. Lee, A.A. Bhagat, P.K. Chaudhuri, D.S. Tan, W.T. Lim, S.C. Lee, P.C. Chen, C.T. Lim, J. Han, Lab Chip 14 (2014) 128–137.
[26] A. Kulasinghe, H. Schmidt, C. Perry, B. Whitfield, L. Kenny, C. Nelson, M.E. Warkiani, C. Punyadeera, Sci. Rep. 8 (2018) 746.
[27] M.E. Warkiani, A.K.P. Tay, B.L. Khoo, X. Xiaofeng, J. Han, C.T. Lim, Lab Chip 15 (2015) 1101–1109.
[28] M.R. Condina, B.A. Dilmetz, S. Razavi Bazaz, J. Meneses, M. Ebrahimi Warkiani, P. Hoffmann, Lab Chip 19 (2019) 1961–1970.
[29] M.S. Syed, M. Rafeie, D. Vandamme, M. Asadnia, R. Henderson, R.A. Taylor, M.E. Warkiani, Bioresour. Technol. 252 (2018) 91–99.
[30] M. Shakeel Syed, M. Rafeie, R. Henderson, D. Vandamme, M. Asadnia, M. Ebrahimi Warkiani, Lab Chip 17 (2017) 2459–2469.
[31] K. Soo-Kyung, C.K. Lee, L. Jae-Chun, R. Kang-In, S. Hun-Joon, K. Tak, Resources Processing 51 (2004) 48–51.
[32] T.R. Vakamalla, V.B.R. Koruprolu, R. Arugonda, N. Mangadoddy, Sep. Purif. Technol. 175 (2017) 481–497.
[33] Z.-S. Bai, H.-L. Wang, S.-T. Tu, Pet. Sci. Technol. 28 (2010) 525–533.
[34] Y. Huang, H.L. Wang, Y.Q. Chen, Y.H. Zhang, Q. Yang, Z.S. Bai, L. Ma, Sci Rep 7 (2017) 2678.
[35] L. Dickey, M. Dallmer, E. Radewonuk, N. Parris, M. Kurantz, J. Craig Jr, Cereal Chem. 74 (1997) 676–680.
[36] J. Yu, Y. Kim, Desalin. Water Treat. 57 (2016) 629–635.
[37] J.-F. Yu, J. Fu, H. Cheng, Z. Cui, Waste Manage. 61 (2017) 362–371.
[38] A. Jank, W. Muller, S. Waldhuber, F. Gerke, C. Ebner, A. Bockreis, Waste Management (New York, N.Y.), 64 (2017) 12–19.
[39] Y. Shi, G. Wells, E. Morgenroth, Bioresour. Technol. 218 (2016) 38–45.
[40] I.C. Bicalho, J.L. Mognon, J. Shimoyama, C.H. Ataíde, C.R. Duarte, Sep. Purif. Technol. 87 (2012) 62–70.
[41] A. Jockwer, R.A. Medronho, R. Wagner, F. Anspach, W.-D. Deckwer, in: Animal Cell Technology: From Target to Market, Springer, 2001, pp. 301–306.
[42] R.C. Pinto, R.A. Medronho, L.R. Castilho, Cytotechnology 56 (2008) 57–67.
[43] E.A. Elsayed, R.A. Medronho, R. Wagner, W.D. Deckwer, Eng. Life Sci. 6 (2006) 347–354.
[44] R. Medronho, J. Schuetze, W. Deckwer, Lat. Am. Appl. Res. 35 (2005) 1–8.
[45] B. Schröder, E.A. Elsayed, J. Olownia, R. Wagner, 2010, 657–664, DOI: 10.1007/978-90-481-3419-9_113.
[46] D. Bradley, The Hydrocyclone, Pergamon Press, Great Britain, 1965.
[47] B. Wang, A.B. Yu, Miner. Eng. 19 (2006) 1022–1033.
[48] L. Svarovsky, in: Solid-Liquid Separation, Fourth Edition, Butterworth-Heinemann, Oxford, 2001, pp. 191–245, DOI: https://doi.org/10.1016/B978-075064568-3/50031-6.
[49] R.H. Perry, Chemical Engineering Handbook, McGraw-Hill, New York, 1984.
[50] K. Rietema, S.I.R. Maatschappij, Chem. Eng. Sci. 15 (1961) 298–302.
[51] S. Schütz, G. Gorbach, M. Piesche, Chem. Eng. Sci. 64 (2009) 3935–3952.
[52] J.M. Martel, M. Toner, Annu. Rev. Biomed. Eng. 16 (2014) 371–396.
[53] S. Razavi Bazaz, N. Kashaninejad, S. Azadi, K. Patel, M. Asadnia, D. Jin, M. Ebrahimi Warkiani, 1900425, Adv. Mater. Technol. (2019).
[54] M.A. Raoufi, S. Razavi Bazaz, H. Niazmand, O. Rouhi, M. Asadnia, A. Razmjou, M. Ebrahimi Warkiani, Soft Matter 16 (2020) 2448–2459.
[55] S. Razavi Bazaz, O. Rouhi, M.A. Raoufi, F. Ejeian, M. Asadnia, D. Jin, M. Ebrahimi Warkiani, Sci. Rep. 10 (2020) 5929.
[56] M. Rafeie, M. Welleweerd, A. Hassanzadeh-Barforoushi, M. Asadnia, W. Olthuis, M. Ebrahimi Warkiani, Biomicrofluidics 11 (2017) 014108.
[57] D. Reinhart, L. Damjanovic, C. Kaisermayer, R. Kunert, Appl. Microbiol. Biotechnol. 99 (2015) 4645–4657.
[58] S.F. Gorfien, W. Paul, D. Judd, L. Tescione, D.W. Jayme, Biopharm. Int. 16 (2003) 34–41.